Journal of the European Ceramic Society 23 (2003) 221–228

www.elsevier.com/locate/jeurceramsoc

Proton-conducting ceramics as electrode/electrolyte materials for SOFC's—part I: preparation, mechanical and thermal properties of sintered bodies

D. Hassan, S. Janes*, R. Clasen

Saarland University, Department of Powder Technology, Im Stadtwald, Building 43, D-66041 Saarbrücken, Germany

Received 8 February 2002; accepted 1 June 2002

Abstract

The aim of these investigations was to prepare and to examine compounds of a high temperature solid oxide fuel cell with a proton conducting electrolyte in view of the mechanical and thermal properties. The powders were made by the conventional solid reaction of carbonates and oxides. The stoichiometry of the electrolyte Ba,Ca niobate (BCN) was varied with $x=0$, $x=0.12$ and $x=0.18$. As potential cathode material $SrCeO_3$ and $SrZrO_3$ stabilised with 5% Yb was prepared, and as anode material cermet of BCN and Ni with 50:50 wt.% was synthesised. The mechanical properties like bending strength (room and high temperature), Young modulus (E), modulus of rigidity (G), Poison's ratio, micro hardness and fracture toughness were measured on sintered samples. The highest values for bending strength, E and G could be found for BCN12 (156 MPa, 160 GPa, 63 GPa) and the cerate (175 MPa, 145 GPa, 56 GPa), the lowest for the cermet BCN/Ni (72 MPa, 68 GPa, 29 GPa). The investigation of the thermal properties of the bulk material showed a thermal stability to a temperature of 1400 °C. The thermal expansion coefficient measured at 1000 °C was found to be in the range of $10–12\times10^{-6}$/K. Further investigations with respect to the mechanical and thermal properties have to be made for the whole system of cathode–electrolyte–anode.

Keywords: Ba (Ca,Nb)O_3; Fuel cells; Mechanical properties; Thermal properties

1. Introduction

As proton conducting ceramics for a high-temperature solid oxide fuel cell (SOFC) barium–calcium–niobate ($Ba_3Ca_{1+x}Nb_{2-x}O_{9-\delta}$) (BCN) is a convenient material for the solid proton conducting electrolyte,[1–8] ytterbium stabilised strontium cerate[9] and strontium zirconate[10] are convenient materials for the cathode (later replaced by LaSr-manganite) and a cermet of BCN and nickel (50:50 mass%) is the convenient material for the anode.

All these materials crystallize in the perowskite structure[11,12] and are well known by their crystal structures and characterised by their conductivity.[13] At the present time, neither the basic knowledge of their mechanical and thermal properties nor of their morphology is very great, so the main intention of this work lay in the measurement of these properties, because there is a direct relationship between the conductivity and the morphology and the size of bulk material and their grain size.

2. Powder synthesis

BCN could be synthesised by two chemical routes: from nitrates, such as $Ba(NO_3)_2$ $Ca(NO_3)_2$ and Nb_2O_5 and from carbonates, such as $BaCO_3$, $CaCO_3$ and Nb_2O_5. We used both methods to prepare BCN-powders.[2–4,8,14] For the powder synthesis by the nitrate route an aqueous solution of barium and calcium nitrate was prepared in which niobium oxide was suspended. The suspension was spray-dried with an inlet temperature of 230–240 °C and an outlet temperature of 130–140 °C, so that spherically shaped particles were obtained. The flow rate was 5 ml/min. Afterwards two calcination steps were necessary to obtain the BCN structure (solid state reaction). Firstly, the powders were

* Corresponding author.
E-mail address: s.janes@matsci.uni-sb.de (S. Janes).

0955-2219/02/$ - see front matter © 2002 Published by Elsevier Science Ltd.
PII: S0955-2219(02)00173-5

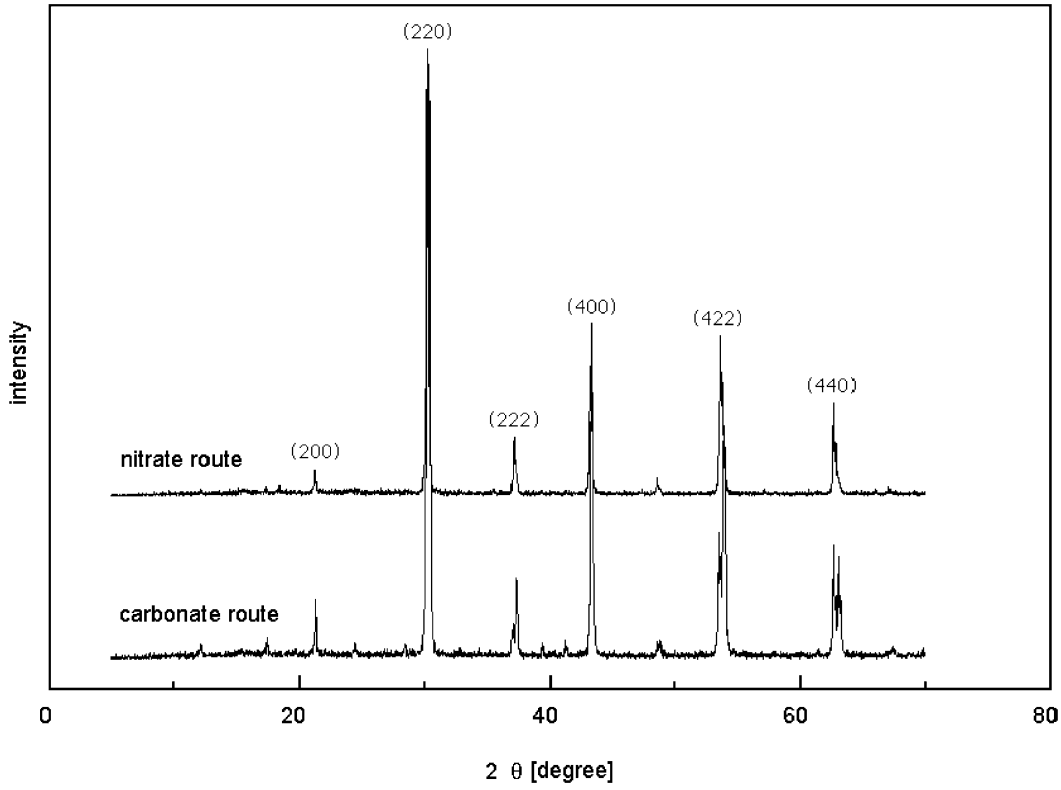

Fig. 1. X-ray diffraction pattern of BCN0 synthesised by nitrate and carbonate route respectively.

heated at 900 °C for 8 h and secondly, at a temperature of 1600 °C for 6 h. X-ray diffractograms do not show peaks other than those of the JCPDS 50–0075 file. This confirms that the synthesised powder was really BCN (Fig. 1).

For the powder prepared by the carbonate route powders of barium and calcium carbonate as well as niobium oxide were mechanically mixed and thermally treated in three steps (solid state reaction). The first thermal treatment was at 1000 °C, the second at 1050 °C both for 10 h, the third was at 1600 °C for 24 h. In the obtained X-ray diffractograms the strong peaks were also identical with those of the JCPDS 50–0075 file. The powder obtained was identified as BCN too (Fig. 1).

With the results of these investigations it was possible to prepare BCN-powder by two different chemical processes. Since then, the carbonate route for preparation of BCN-powder has been preferred due to its better yield.

The synthesis of the cerate and zirconate powders has also been done by solid state reaction of the carbonate route. In the case of cerates powder was synthesised from strontium carbonate and cerium oxide and for the zirconates strontium carbonate and zirconia powders respectively in the same way as described for the synthesis of BCN. The two calcination steps were 1300 and 1400 °C both for 10 h. The powders were identified by X-ray diffractograms as seen in Figs. 2 and 3. Fig. 2 shows the X-ray diffractogram of strontium cerate samples after the two calcination steps and after sintering at 1600 °C. The main peaks of the diagram are identically with those of the JCPDS 23-1412 file, so that the resulted powders are realy strontium cerate. The X-ray diffractogram of strontium zirconate is shown in Fig. 3. Here also we find only the peaks of strontium zirconate compared to the JCPDS 44-161 file.

3. Preparation of test samples

The synthesised powders were uniaxial pre-pressed and cold isostatical pressed to stacks of $40\times10\times10$ mm^3. The pressure for the uniaxial pressing was in the range of 60–100 MPa, for the cold isostatic pressing between 400 and 800 MPa. For the mechanical measurements like three-point bending test, the stacks were sintered as a function of sintering temperature in the range of 1400–1650 °C. Afterwards the sintered parts were sawn in samples of $30\times4\times3$ mm^3 and polished. For four-point bending test the samples have had a dimension of $40\times4\times3$ mm^3 and were prepared in the same way as described before.

Differential thermal analysis (DTA) and differential thermal gravimetry (DTG) measurements have been done on fractured specimens of the sintered samples. The weight of the samples was between 50 and 70 mg. The reference material was dried sintered alumina.

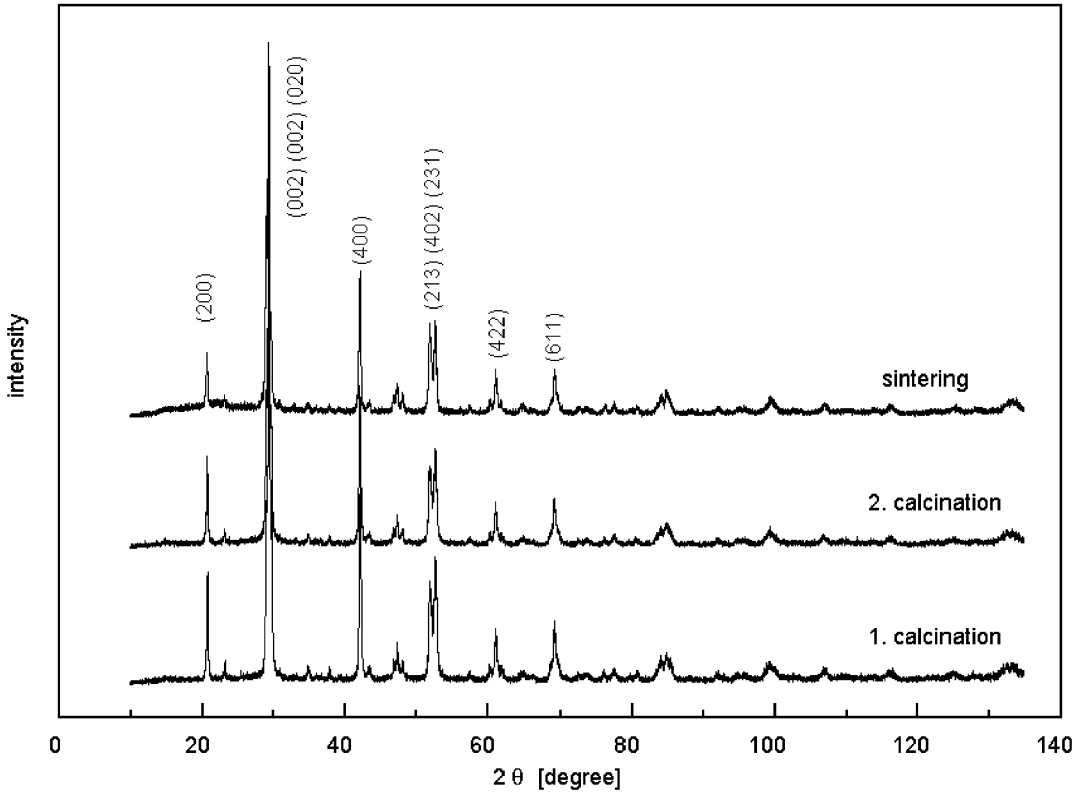

Fig. 2. X-ray diffraction pattern of $SrCeO_3$ (5% Yb).

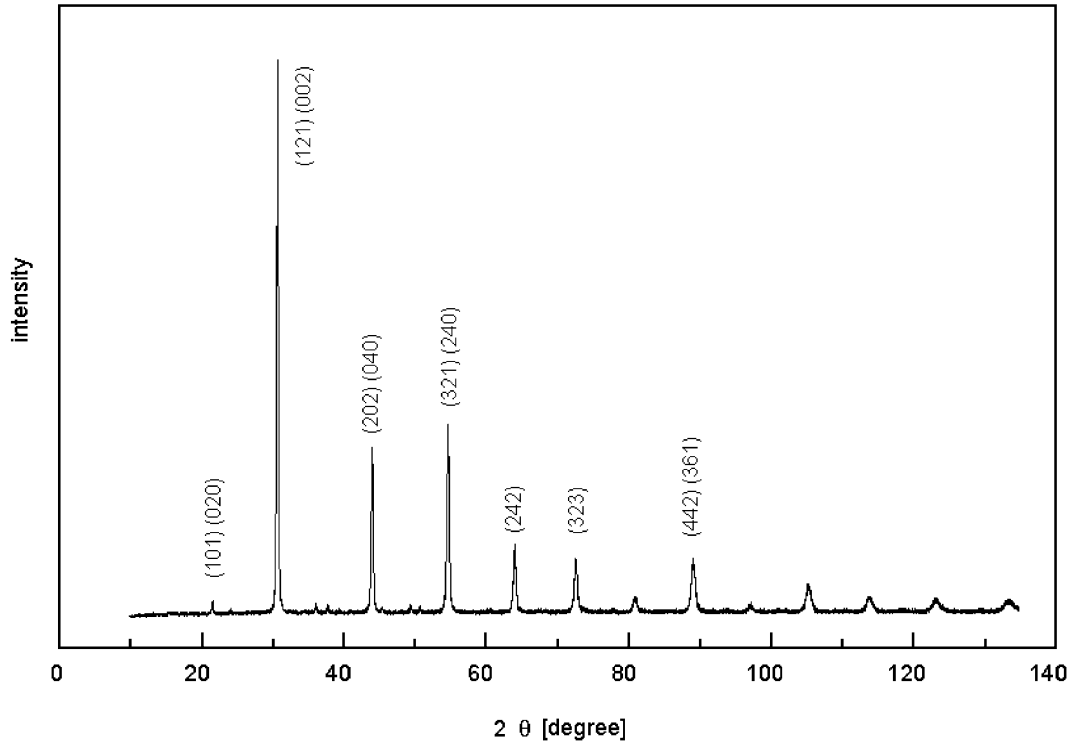

Fig. 3. X-ray diffraction pattern of $SrZrO_3$ (5% Yb).

Dilatometry was made once on green bodies for examination the sintering behaviour and once on sintered samples with a length of 20 mm to measure the coefficient of expansion.

4. Mechanical properties

The mechanical properties were examined due to bending strength at room temperature and higher temperatures, Young's modulus (E), modulus of rigidity (G), Poison's ratio, fracture toughness and micro hardness by Vickers.

The results of the three-point bending test at room temperature for the different electrode/electrolyte materials were concluded in Table 1. Thereby BCN0 means the stoichiometric composition with $x=0$, while BCN12 and BCN18 has a variation of $x=0.12$ and $x=0.18$. The greatest value of 175 MPa maximum bending strength was achieved by the 5% Yb-stabilised $SrCeO_3$, followed by BCN12 (156 MPa), BCN18 (121 MPa), BCN0 (106 MPa), the cermet BCN/Ni (72 MPa) and 5% Yb-stabilized $SrZrO_3$ (66 MPa). $SrCeO_3$ possess the greatest value of strength, while BCN18 has the smallest range of variation.

Therefore, for BCN18 materials only four-point bending tests were performed in a temperature range between 700 and 1000 °C. The results are shown in Table 2. In the range of temperatures from 700 to 900 °C the hot bending strength is nearly constant, while at 1000 °C the strength of BCN18 increase of about twice in maximum.

The moduli were calculated by the ultrasonic method on sintered stacks where the pulse relaxation of ultrasonic through the samples was measured. The results are summarised in Table 3. In the case of elastic modulus (E) and modulus of rigidity (G) the greatest values were found with the BCN0 (162 GPa; 65 GPa) followed by BCN12 (160 GPa; 63 GPa) and BCN18 (148 GPa; 60 GPa). A little bit lower values were achieved with $SrCeO_3$ (145 GPa; 56 GPa) and the $SrZrO_3$ (131 GPa; 52 GPa). The cermet BCN/Ni only has values of 68 and 29 GPa.

The results of the micro hardness (Vickers) combined with fracture toughness K_{Ic} are summarised in Table 4. In this case the micro hardness of all tested materials is nearly in the same order, except the cermet BCN/Ni. The same results were achieved of fracture toughness by using the micro hardness test.

5. Thermal properties

The temperature stability of the powders and sintered ceramics was examined by differential thermal gravimetry (DTG) and differential thermal analysis (DTA) measurements (Figs. 4–6). In Figs. 4–6 DTG-measurements of BCN, cerates and zirconates result, that the materials are stable in the measured temperature range up to 1400 °C.

The sintering behaviour of green bodies was measured by dilatometry. In the case of BCN the starting temperature for sintering was about 1400 °C as seen in Fig. 7. The thermal expansion coefficient α was determined on

Table 1
Bending strength and density of electrode/electrolyte materials

Material	Bending strength (MPa)	Density (% TD)
BCN0	102–106	98
BCN12	96–156	~100
BCN18	96–121	99
$SrCeO_3$, 5% Yb	128–175	~100
$SrZrO_3$, 5% Yb	31–66	98
BCN/Ni	36–72	~100

Table 2
Hot bending strength of BCN18

Temperature (°C)	700	800	900	1000
Hot bending strength (MPa)	34	35	34	52
	42	52	52	59
				66
				99

Table 3
Moduli and Poison's ratio of electrode/electrolyte materials

Material	E (GPa)	G (GPa)	Poison's ratio μ
BCN0	137–162	55–65	0.25
BCN12	152–160	60–63	0.27
BCN18	140–148	56–60	0.25–0.27
$SrCeO_3$, 5% Yb	145	56	0.30
$SrZrO_3$, 5% Yb	131	52	0.25
BCN/Ni	68	29	0.19

Table 4
Vickers hardness (HV) and fracture toughness (K_{IC}) of electrode/electrolyte materials

Material	HV (GPa)	K_{IC} (MPa m$^{-1/2}$)
BCN0	4.8–5.7	0.78–0.95
BCN12	5.9–6.4	0.71–0.84
BCN18	4.5–5.4	0.91–1.10
$SrCeO_3$, 5% Yb	5.5	2.08
$SrZrO_3$, 5% Yb	4.6	1.54
BCN/Ni	1.0	1.0

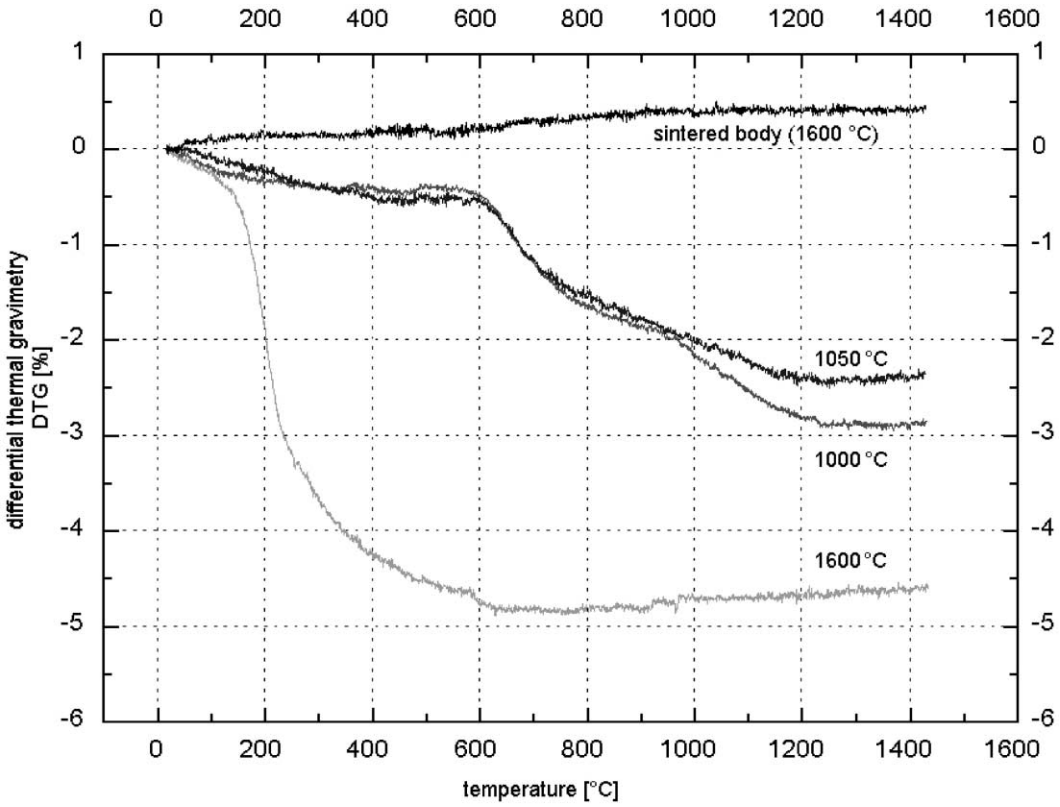

Fig. 4. Differential thermal gravimetry diagram of BCN18.

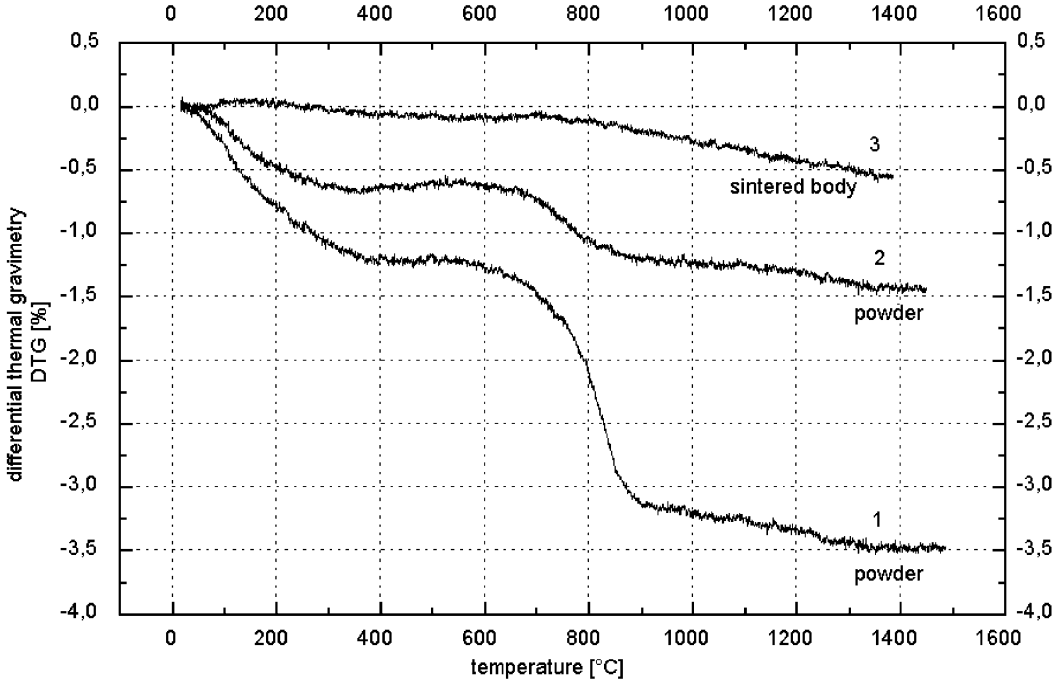

Fig. 5. Differential thermal gravimetry diagram of $SrCeO_2$ (5% Yb).

sintered bodies at the same device. The results are reported in Table 5 for the different electrode/electrolyte materials. Thermal expansion coefficients of all tested materials are nearly in the same range of $10.3–12.4\times10^{-6}$/K between ambient temperature and 1000 °C.

6. Ceramographic investigations

The microstructure of the sintered bodies was prepared by traditional ceramographic methods (sawing, grinding and polishing with diamond tools) and the

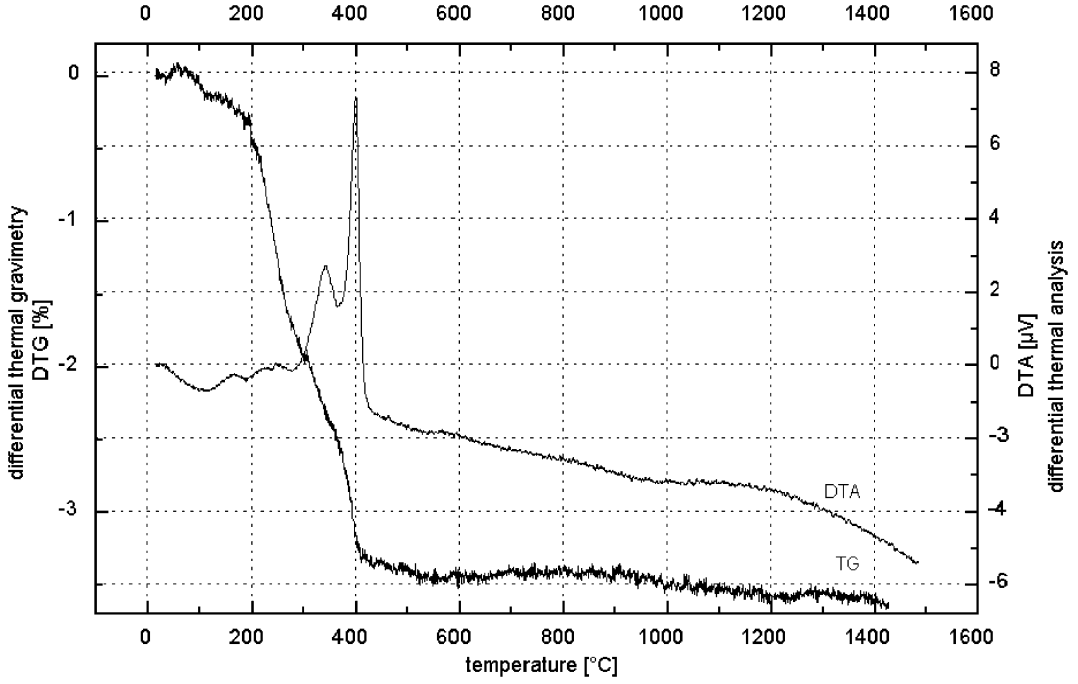

Fig. 6. Differential thermal gravimetry and differential thermal analysis diagrams of $SrZrO_3$ (5% Yb).

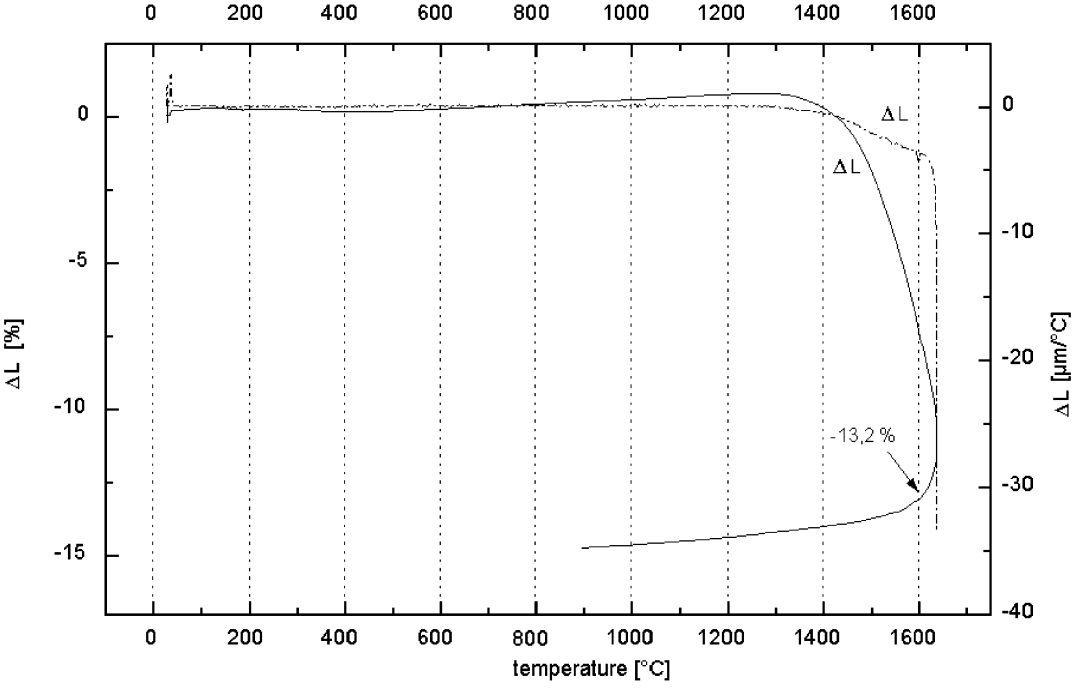

Fig. 7. Dilatometric measurement of a BCN18 green body.

Table 5
Thermal expansion coefficient of electrode/electrolyte materials

Material	(10^{-6}/K)
BCN0	10.3–11.7
BCN12	10.9–12.1
BCN18	12.3
$SrCeO_3$, 5% Yb	11.5–12.0
$SrZrO_3$, 5% Yb	10.4

grinding tests were investigated by Scanning Electron Microscopy (SEM).

Figs. 8–11 show micro graphs of all tested materials. In Fig. 8 the fracture surface of a BCN 18 sample is seen. The micro picture shows a very dense structure without pores. The shell shaped morphology also indicates that the sample structure is very dense so that the fracture occurs trans-granules, that means, through the grains. The grain size is in the range from 1 to 5 μm.

In order to achieve high values of electric conductivity of the electrolyte it is of interest that the electrolyte structure consists of a small numbers of great grains so that the grain boundary is minimised. Therefore the sintered BCN samples were thermally treated at 1500 °C for 24 h (thermal etching). Afterwards the grain size of the etched samples were in the order of 12–23 μm. Fig. 9 shows a micro pictures of a thermal etched BCN sample.

The SEM picture of sintered $SrZrO_3$ (5% Yb stabilised) is to be seen in Fig. 10. The micro graph shows a porous structure with a particles size of 0.5–2 μm. In Fig. 11 the SEM picture of $SrCeO_3$ (5% Yb stabilised) is shown. Here a glassy, nearly dense surface structure of a fracture micro picture with only small sized pores can be recognised.

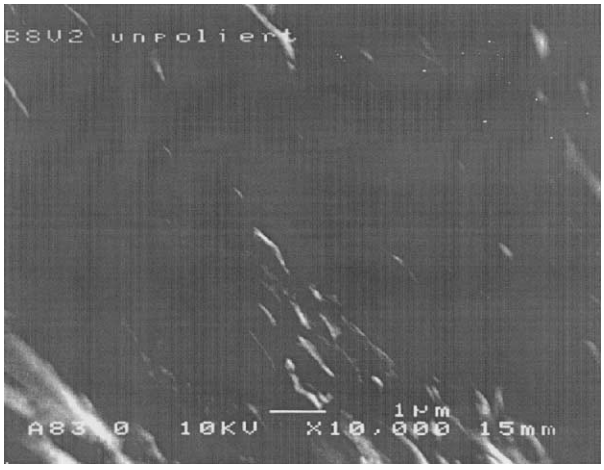

Fig. 8. SEM picture of a BCN18 sintered sample (fracture surface).

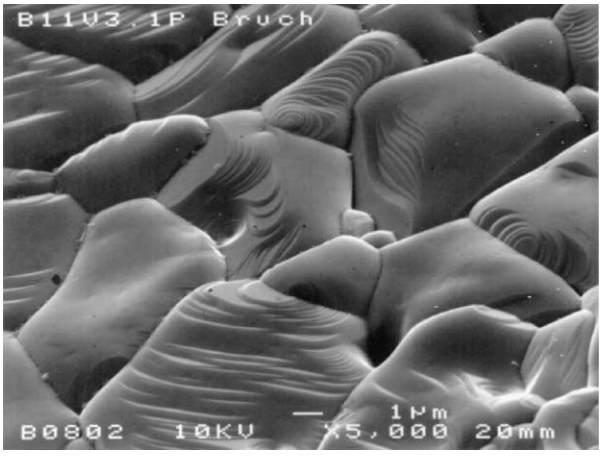

Fig. 9. SEM picture of a sintered and thermal etched BCN18 sample (fracture surface).

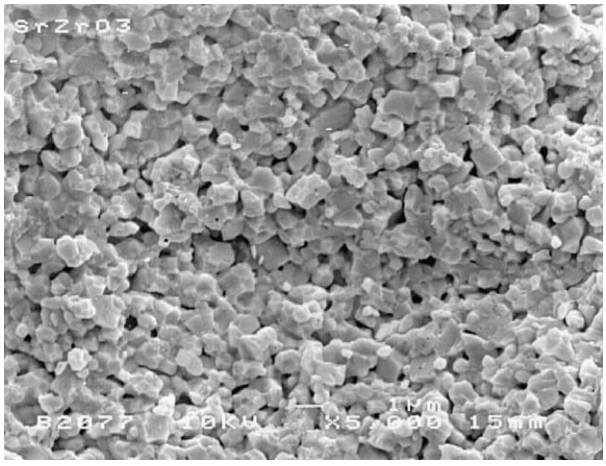

Fig. 10. SEM picture of a sintered $SrZrO_3$ (5% Yb) sample.

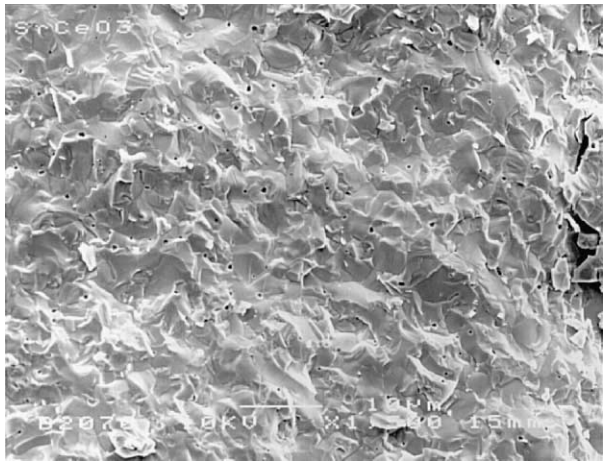

Fig. 11. SEM picture of a sintered $SrCeO_3$ (5% Yb) sample.

7. Discussion

All the examined materials for the electrodes or the electrolyte in a high temperature proton conducting solid oxide fuel cell (SOFC) seem to be potential candidates for a later use in the SOFC.

The powders were synthesised by the nitrate and carbonate route and solid state reaction. In both cases the final products were achieved. The carbonate route will be preferred due to its better yield.

In the group of BCN with $x=0$ to $x=0.18$, the highest values of the bending stress were found for BCN12 followed by BCN18 and BCN0. These correlate with the density. It could be shown that the calcination and the sintering conditions do not influence the bending strength. Beside this, the morphology can affect the bending strength, but the values can be correlated with the homogeneity of the sintered samples. The same correlation between bending strength and density which was found for BCN was observed for tother materials like cerate and zirconate. By means of a SEM picture of sintered zirconate (Fig. 10) the low bending stress can be explained. It shows many pores and the particle size lays between 0.5 and 2 μm, but the rupture surface of the cerate sintered body is dense. This can be seen in Fig. 11.

The results of the four-point hot bending test are only single point measurements because the preparation of the sample was, due to the large size of the stacks, not so easy and a lot of faults appeared. Therefore these results shoud not be overestimated. The bending strength of BCN18 at 1000 °C can be compared with the bending strength of BCN at room temperature. The same tendency of the electrode/electrolyte materials as the bending strength can be found for the other measured mechanical properties with highest values for the cerate and lowest values for the cermet due to the described reasons.

The TG measurements lead to assumption that these materials can be applied in a SOFC, which works in an aspect working temperature range of 600–800 °C, because all these materials are stable in this temperature range. The measurement of the expansion coefficient showed that the values are all at the same range and thus a system of anode–electrolyte–cathode can be constructed with these materials.

Acknowledgements

We wish to acknowledge and to thank the Deutsche Forchungsgemeinschaft (DFG) for the financial support of these investigations, which were performed in the Schwerpunktprogramm ''Multifunktionswerkstoffe'.

References

1. Schober, T., Proton conductivity at high temperatures in oxidic perovskites. *IFF-Bulletin* 1994, **45** (Preface).
2. Mono, T., Meuffels, P., Triefenbach, D. and Schober, T., Synthesis and characterization of high temperature proton conductors of type $Ba_3Ca_{1-x}Nb_{2-x}O_{9-a}$. *Ionics*, 1995, **1**, 469.
3. Mono, T., *Keramische Protonenleiter des Systems BaCaNbO*. PhD thesis, Forschungszentrum Jülich, RWTH Aachen, Aachen, Germany, 1997.
4. Zimmer, E., Scharf, K., Mono, T., Friedrich, J. and Schober, T., Preparation of the high temperature proton conductor $Ba_3Ca_{1.18}Nb_{1.82}O_{8.73}$ via a wet chemical route. *Solid State Ionics*, 1997, **97**, 505–509.
5. Mono, T. and Schober, T., Lattice parameter change in water vapor exposed $Ba_3Ca_{1.18}Nb_{1.82}O_{9-a}$. *Solid State Ionics*, 1996, **91**, 155–159.
6. Bohn, H. G., Schober, T., Mono, T. and Schilling, W., The high temperature proton conductor $Ba_3Ca_{1.18}Nb_{1.82}O_{9-x}$, I. Electrical conductivity. *Solid State Ionics*, 1999, **117**, 219–228.
7. Schober, T., Bohn, H. G., Mono, T. and Schilling, W., II. Electrochemical cell measurements and TEM. *Solid State Ionics*, 1999, **118**, 173–178.
8. Hassan, D., *Herstellung und Charakterisierung einzelner Komponenten einer protonenleitenden Hochtemperaturbrennstoffzelle (SOFC)*. PhD thesis, Saarland University, Saarbrücken, Germany, 1998.
9. Krug, F. and Schober, T., In situ measurements of the water uptaken in Yb doped $SrCeO_3$. *Solid State Ionics*, 1996, **92**, 297–302.
10. Smith, J. S. II, Dolloff, R. T. and Mazdiyasni, K. S., Preparation and characterization of alkoxy-derived $SrZO_3$ and $BaTiO_3$. *J. Am. Ceram. Soc.*, 1970, **53**, 91–95.
11. Lind, K., *Festkörperphysikalische Methoden zur Untersuchung von protonenleitenden Oxidkeramiken*. PhD thesis Saarland University, Saarbrücken, Germany, 1998.
12. Altmayer, M., *Aufbau und Inbetriebnahme einer Hochtemperatur-Brennstoffzelle auf der Basis oxidischer Hochtemperatur-Protonenleiter*. PhD thesis Saarland University, Saarbrücken, Germany, 1997.
13. Marion, S., *Impedanzspektroskopie an protonenleitenden Keramiken*. PhD thesis Saarland University, Saarbrücken, Germany, 1997.
14. Bausch, S., *Impedanzanalyse und mechanische Relaxation von keramischen Protonenleitern*. PhD thesis, Forschungszentrum Jülich, RWTH Aachen, Aachen, Germany, 1997.